VALIDATION ON INTRALAMINAR BEHAVIOR OF THE ENHANCED DAMAGE LMT-MESOMODEL

A.C. Galucio[1], P.M. Mohite[2], G. Lubineau[3] and P. Ladevèze[3,4]

[1]EADS Innovation Works, Suresnes, France
[2] Indian Institute of Technology Kanpur, Dept. of Aerospace Engineering, India
[3] LMT-Cachan (ENS-Cachan/Paris 6 univ./CNRS/UniverSud Paris), Cachan, France
[4] EADS Foundation Chair in "Advanced Computational Structural Mechanics"
lubineau@lmt.ens-cachan.fr, ladeveze@lmt.ens-cachan.fr

ABSTRACT

The enhanced version of the damage mesomodel for laminates (DML) introduced at the LMT-Cachan is validated and illustrated for the intralaminar damage by using User-MATerial subroutines in Abaqus Std. In order to show the effectiveness of the proposed model, an identification phase is outlined followed by preliminary results based on an industrial test-case. The identification is carried out for basic tests like 0° traction/compression tests, traction on $[0_m/90_n]_s$ laminates, monotonic and cyclic traction tests on $[\pm 45]_{4s}$ and $[\pm 67.5]_{4s}$ laminates. The damage intralaminar mechanisms validated in this study are: fiber breaking, diffuse damage and matrix microcraking. The validation test is carried out for an actual industrial lay-up: 32-ply laminate with a central open hole. It is found that the present DML succeeds in predicting the evolution and propagation of the above mentioned damage mechanisms until final fracture.

1. INTRODUCTION

The damage mesomodel for laminates (DML) has been developed over last 20 years, particularly at LMT-Cachan [1]. The DML is based on three key points: (i) the use of the mesoscale – the intermediate scale between the structure (macro) and the constituents (micro) – the laminate is thus assumed to be divided into two elementary constituents which are continuous media on the meso scale: the ply [2] and the interface [3]; (ii) internal variable approach using damage indicators which are assumed to be homogeneous throughout the thickness of the elementary ply; and (iii) method of local states – which relates the thermodynamic forces to the damage.

The present DML has been improved over recent years in the light of micromechanics for various mechanisms of degradation, more specifically for transverse cracking and local delamination [4][5]. The enhanced model is compatible with classical works in micromechanics [6][7] and extends them to general structure computation. An interesting feature of that enhanced version is that there is a separate damage indicator for each degradation mechanism. The present DML can characterize the following damage mechanisms: (1) fiber fracture (2) matrix microcracking (3) matrix diffuse damage and (4) delamination. Furthermore, it gives the evolution of these damage mechanisms until final fracture keeping all calculations in the mesoscale. For localization and dynamic loading, the damage mesomodel with delay effect, proposed by [8], has been used. The mesomodel has been identified against classical tests.

In the present study, no attempt has been made to validate the mesomodel for interlaminar behaviour. First, validation is leading on basic identification samples. A more complex comparison is then performed in the framework of a thick holed sample under traction.

2. DAMAGE MESOMODEL FOR PLY

The enhanced damage mesomodel is not recalled here. Detailed equations including the complete description of micro cracking from micromechanical homogenization can be found in [9][10].

We just emphasize that each intra laminar mechanism of degradation is fully described by independent damage indicators: fiber breaking / diffuse damage (with separated indicators in the transverse and in the shear direction) / transverse cracking (for which indicators are related to the underlying micro cracking rate by using micro meso relations) / plasticity, which is written thanks effective quantities.

The proposed mesomodel can be easily implemented within the framework of commercial finite element softwares. The model has been previously introduced in Abaqus/Std using User subroutines. Details concerning key choices for the implementation can be found in [9][11]. These developments are directly reused here.

3. IDENTIFICATION

The aim of that part is the validation and illustration of both model and implementation in the case of intralaminar degradation. The interlaminar behavior has also been introduced in the FE software but is out of the scope of that work.
Material is for all examples a T700/M21 carbon-epoxy composite provided by EADS-IW, which has also been in charge of the experimental characterization.

3.1 0^0 Traction test

Two main keypoints are reproduced correctly by the proposed model: (1) the non-linearity with the increasing loading (2) the ultimate load. For these materials, apparent young modulus can indeed increase up to 20 per cent due to the alignment of the fibers during the traction. That point is reproduced in the model by a longitudinal modulus related to the longitudinal strain. As illustrated Figure 1, ultimate load is also correctly predicted.

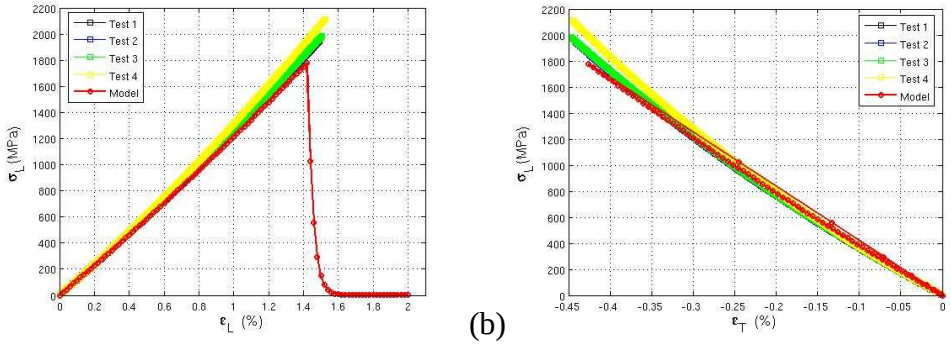

(a) (b)

Figure 1: Validation for fiber breaking in traction: (a) Longitudinal stress vs longitudinal strain (b) Longitudinal stress vs transverse strain.

3.2 0^0 Compression test

Similar to the traction test, the model is here validated for the fiber fracture and non-linear behavior in compression. The longitudinal stress vs longitudinal strain and transverse strain are shown in Figure 2 (a) and (b), respectively. It has to be noted that

model is validated for test for which the ultimate load is minimum. It is clear that the model is in reasonable agreement the experimental investigations. The difference in the longitudinal stress vs transverse strain can be explained by experimental difficulties and defects of compression test.

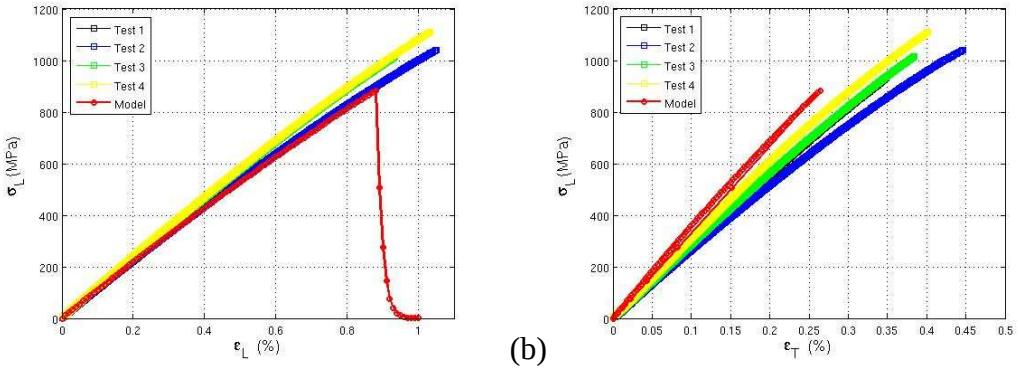

Figure 2: Validation for fiber breaking in compression: (a) Longitudinal stress vs longitudinal strain (b) Longitudinal stress vs transverse strain.

3.3 $[0_m/90_n]_s$ traction test for microcracking

Two laminate sequences - $[0_4/90_4/0_4]$ and $[0_4/90_{12}/0_4]$ - are studied. One investigates the relation between the mean traction stress and the micro cracking level which is quantified as for classical micromechanical analysis by a micro cracking density [6][7]. It should be noted that the enhanced mesomodel provides not only damage indicators but also relations between these damage indicators and underlying morphology. It thus differs and provides stronger information than classical damage approaches [12].

Figure 3 (a) and (b) illustrates development of cracking density and fiber damage for the two sequences. As far as microcracking is concerned, predictions are really reasonable if one considers the strong variability, which is often observed for that kind of experiment. Sample breaking appears at the same level for experiments and numerical simulation, with a microcracking density around .5 before final breaking.

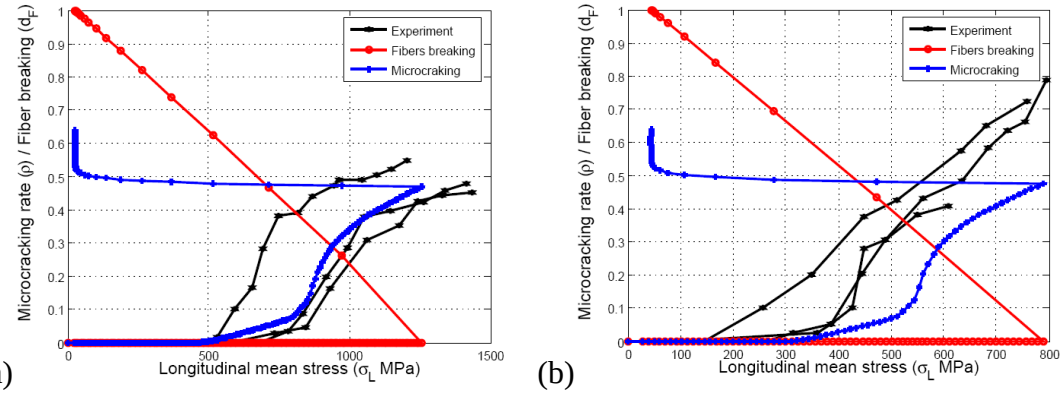

Figure 3: Validation for matrix microcracking in monotonic traction: (a) $[0_4/90_4/0_4]$ (b) $[0_4/90_{12}/0_4]$.

3.4 $[\pm 45]_{4s}$ cyclic traction test

Here, the monotonic cyclic traction test is carried out on $[\pm 45]_{4s}$ laminate. Such a test is in fact a shear experiment, which is characterized by a large level of plasticity and very

few micro cracks except around the final breaking. Diffuse damage is the main degradation mechanism [13].

The shear stress/strain curve is provided Figure 4 (a), and a detailed view of the starting of the curve is given Figure 4(b). It is clear that the simulated stress/ strain curve overlaps the experimental one for low loads. The divergence between simulation and experiment for moderate and high load levels has not to be associated to a limitation of the model, but rather to the fact that large rotations of the fibers have not been considered here. Previous studies have already illustrated the major influence of fiber rotation during shear test investigation.

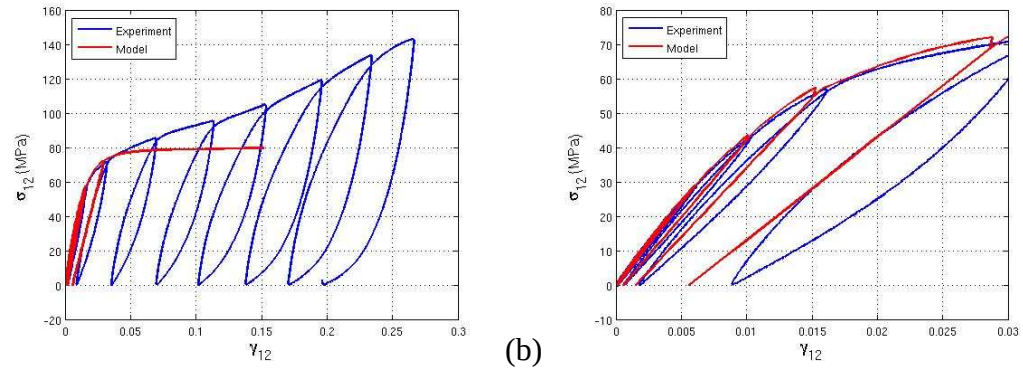

(b) (b)

Figure 4: Validation for shear modulus, shear diffuse damage and plasticity parameters in cyclic traction (a) shear stress vs shear strain (b) exploded view of (a).

3.5 $[\pm 67.5]_{4s}$ traction test

That test is used for the validation of both plasticity and damage under coupled transverse/shear loading. Figure 5(a) provides the comparison between experimental/numerical curves for sample longitudinal load vs. longitudinal strain (note that the experimental curve is just provided until 4000N which is not the experimental ultimate load). The comparison is reasonable. The experimental ultimate load is given to be 5500 N whereas the model predicts the failure around 5700 N. Further, the Figure 5(b) shows the variation of global longitudinal force vs microcracking rate. The microcracking develops at the experimental force value of 4400 N whereas the model predicts the initiation of microcracking at the force value of 4700 N. An interesting key point is the failure mechanism of the sample, which is due to a localized and strong increasing of micro cracking density for the simulation. Experimentally, that kind of sample also fails by a localisation mechanism, since the first transverse cracks immediately collapse through the entire thickness of the laminates.

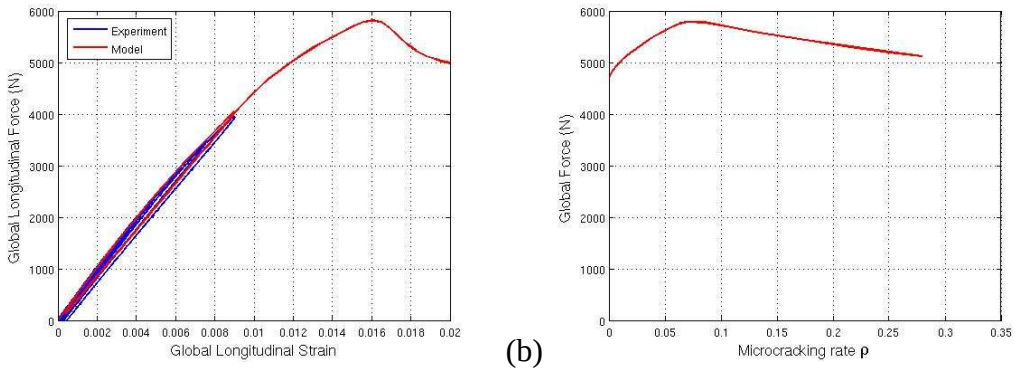

(a) (b)

Figure 5: Validation for (a) plasticity parameters (cyclic traction) (b) microcracking (monotonic traction) initiation.

4 VALIDATION

In this section, preliminary results of validation are presented based on an industrial test-case. In this regard, a 32-ply laminate of sequence $[0/-45/90_2/45/90_2/-45/90/45/90_2/-45/0/45/90]_s$ with an open central hole under monotonic traction is studied. Due to symmetry in the thickness direction, the mesh can be reduced to one half of the sample. For didactical purposes, plies are numbered from 0 to 12, starting from the 90 central ply towards the 0 skin ply. Of course, according to the primary hypothesis of the mesomodel, multiple plies (as 90_2 for example) are considered as single layers with larger thickness.

Herein, 75% of fracture load is applied in traction to the specimen. The global fracture of the laminate occurs at 2.3 mm of displacement loading. All the results presented in this section are for this load-unload cycle. The post-mortem specimen is shown in Figure 6 (a) and (b).

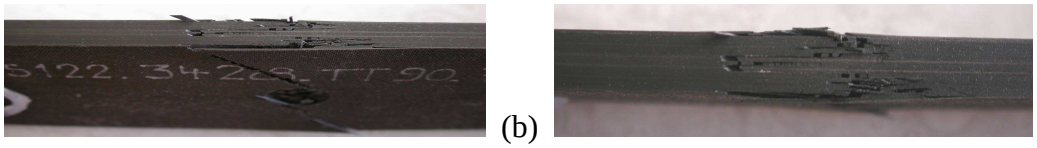

(a) (b)

Figure 6: Fractured specimen of 32-plies laminate with an open hole under monotonic traction (Source: Centre D'Essai Aéronautique de Toulouse).

4.1 Fiber fracture

Several damage maps for the fiber fracture are shown in Figure 7. Figure 7(a) shows the fiber breaking in 0^0 ply near the core of the laminate (Ply No. 2). Figure 7(b) and (c) shows the fiber breaking in 45^0 (Ply No. 9) and -45^0 ply (Ply No. 11), respectively and (d) shows the fiber breaking in 0^0 ply at the top of the laminate. From Figure 7(a), (d) and Figure 6(a), (b) the present model seems to predict the fiber breaking accurately. Especially, effect of the orientation of adjacent plies seems to be taken into account.

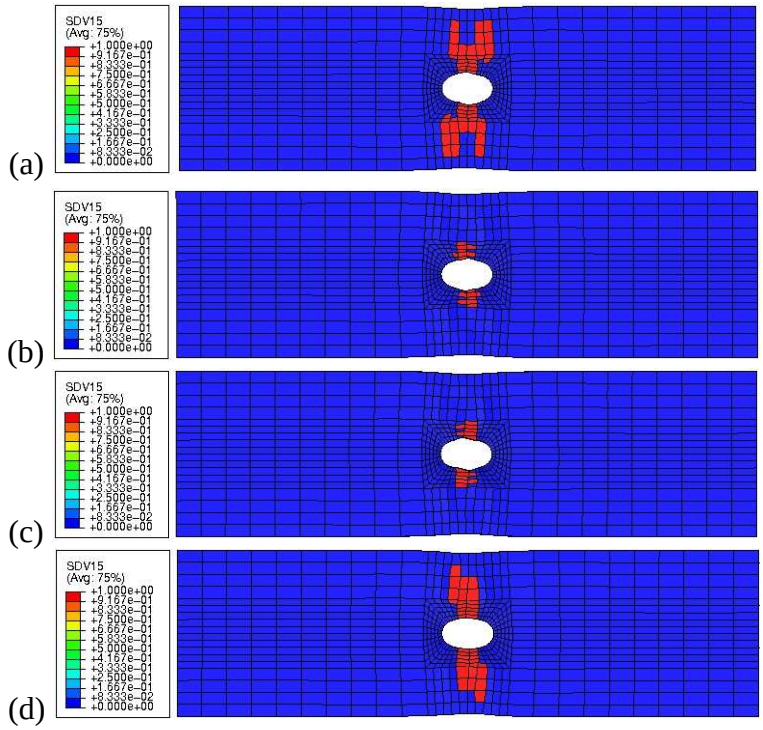

Figure 7: Validation for fiber breaking (a) Ply No. 2 (0^0 Ply), (b) Ply No. 9 (45^0 Ply) (c) Ply No. 11 (-45^0 Ply) and (d) Ply No. 12 (0^0 Ply).

4.2 Matrix micro cracking

The X-ray radiograph for matrix microcracking in 90^0 laminae is shown in Figure 8. This X-ray radiograph was obtained at the 90% of fracture load. The damage maps for microcracking rate obtained by the model at the maximum load of 75% of fracture load are shown in Figure 9. Figure 9(a) and (b) shows the microcracking rate in 90^0 ply at the core (Ply No. 0) and near the skin (Ply No. 10). The micro cracking shape in both 90^0 laminae are in good accordance with the experimental results. The intensity of the microcracking and the area of microcracking are also in accordance with the experimental results.

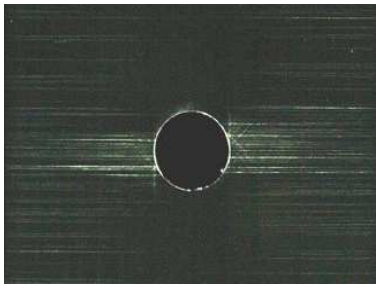

Figure 8: Experimental result for matrix microcracking in 90^0 Ply (Source: Centre D'Essai Aéronautique de Toulouse).

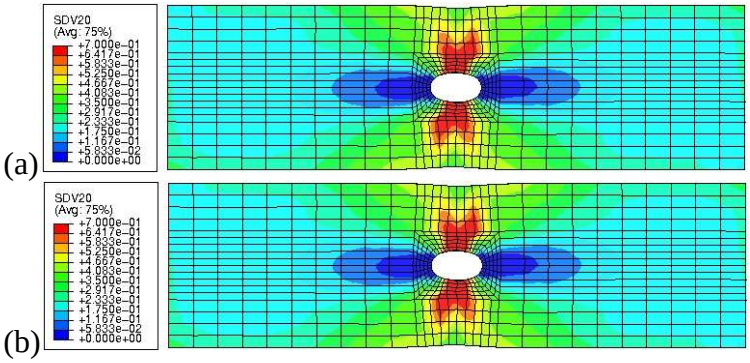

Figure 9: Validation for matrix microcracking (a) Ply No. 0 (90^0 Ply) and (b) Ply No. 10 (90^0 Ply).

5. CONCLUSIONS

The enhanced damage mesomodel based on underlying micro-meso relations, and implemented in Abaqus/Std in previous works, is validated with various experimental results for the material T700/M21. The key points of this validation study are:

1. The traction and compression fracture of the fibers is correctly captured by the present mesomodel. The non-linear behavior both in traction and compression is also accurately predicted.
2. Simple identification experiments (shear – transverse loading – coupled shear/transverse loading) are well predicted. Additionally, this approach reproduces both the correct global curve and the correct temporal and spatial scheme for the damage mechanism development.
3. The current approach seems to be efficient for the simulation of industrial identification sample, at least for the illustration example.

Thus, the present version of the enhanced damage mesomodel has been validated for intralaminar damage mechanisms. Coming further exhaustive works are related to the validation for industrial tests including interlaminar damage and different composite materials.

REFERENCES

[1] P. Ladevèze (1992). **A damage computational method for composite structures**, *Computers and Structures.* v. 44. 79–87.

[2] P. Ladevèze and E. Le Dantec (1992). **Damage modelling of the elementary ply for laminated composites**. *Composite Science and Technology*. v. 43. 257-267.

[3] O. Allix and P. Ladevèze (1992). **Interlaminar interface modelling for the prediction of delamination.** *Composite Structures*, v. 22(4). 235–242.

[4] P. Ladevèze and G. Lubineau (2001). **On a damage mesomodel for laminates: micro-meso relationships, possibilities and limits.** *Compos Sci Technol*. v. 61(15). 2149-2158.

[5] P. Ladevèze, G. Lubineau and D. Marsal (2006). **Towards a bridge between the micro- and the mesomechanics of delamination for laminated composites**. *Composites Science and Technology*. v. 66(6). 698–712.

[6] J. Nairn and S. Hu (1994). **Matrix microcracking**. *In Taljera, editor, Damage Mechanics of Composite Materials*. 187–243.

[7] J.-M. Berthelot (2003). **Transverse cracking and delamination in cross-ply glass-fiber and carbon-fiber reinforced plastic laminates: Static and fatigue loading**. *Appl. Mech. Rev.*, v. 56. 111–147.

[8] P. Ladevèze, O. Allix, J.-F. Deü and D. Lévêque (2000). **A mesomodel for localization and damage computation in laminates**. *Comput Methods Appl Mech Engrg*. v. 183. 105-122.

[9] G. Lubineau and P. Ladevèze (2007). **Construction of a micromechanics-based intralaminar mesomodel and illustrations in ABAQUS/Standard**. *Comput Mater Sci*. Article in Press. *Available online.*

[10] G. Lubineau (2008). **A pyramidal modelling scheme for laminates – identification of transverse cracking -**. *International Journal of Damage mechanics.* Submitted.

[11] G. Lubineau and P. Ladevèze (2008). **A pyramidal modeling for laminates composites – Illustrations Using Abaqus-** *49th SDM Conference. American Institute of Aeronautics and Astronautics.*

[12] I. Lapczyk and J.A. Hurtado (2007). **Progressive damage modeling in fiber-reinforced materials**. *Composites Part A*. v. 38. 2333-2341.

[13] F. Lagattu, M. Lafarie-Frenot (2000). **Variation of PEEK matrix crystallinity in APC-2 composite sub jected to large shearing deformation**. *Composite Science and Technology. v.* 60. 605–612.